WILEY

Research Article

Advancing Energy Performance Efficiency in Residential Buildings for Sustainable Design: Integrating Machine Learning and Optimized Explainable AI (AIX)

Badr Saad Alotaibi [ORCID]

Architectural Engineering Department, College of Engineering, Najran University, 66426 Najran, Saudi Arabia

Correspondence should be addressed to Badr Saad Alotaibi; bsalotaibi@nu.edu.sa

Buildings play a critical role in energy consumption, representing one of the primary consumers of power. Heating load (HL) and cooling load (CL) are essential for determining the energy efficiency of buildings. Several research projects attempt to address the critical challenge of enhancing energy efficiency in residential buildings, focusing on accurately estimating HL and CL using solutions that implement statistical prediction or typical building control management. This study, however, looked into advanced machine learning (ML) models for sustainable building design based on harnessing the potential of artificial intelligence and explainable AI (AIX) technologies. The proposed model was trained and tested using a dataset of 768 buildings based on feature engineering methods with various ML algorithms (including cutting-edge emotional neural learning (ENN), nonparametric kernel-based probabilistic models known as Gaussian process regression (GPR), and boosted tree (BT) algorithm). In addition, the output of the model was fed to standard building energy performance software (Ecotect) that utilizes the dataset from twelve different building shapes to perform various building energy efficiency analyses. The overall performance of the proposed model was measured using different performance metrics, including MAPE, MAE, RMSE, and PCC to measure the performance of HL- and CL-based building energy efficiency. The performance evaluation results indicate that the M3 variants, especially GPR-M3, consistently outperformed their counterparts across heating and cooling scenarios. The three models indicated reliability for modeling HL and CL. However, for HL, the GPR-M3 model emerged as the best model, outperforming GPR-M1 by 9.2% and GPR-M2 by 3.9%. Similarly, GPR-M3 is superior to CL, with the highest PCC at 0.9858, marking an 8.1% and 1.9% improvement over GPR-M1 and GPR-M2, respectively.

1. Introduction

In today's climate, the discourse addressing residential energy consumption has moved beyond a mere conversation about conserving resources. It now stands as a vital component in the global machinery working towards sustainable living and environmental preservation [1]. In light of escalating energy prices, growing environmental concerns, and a global shift towards sustainable design, the demand for energy-efficient buildings is reaching new heights. Given that they are the cause of a considerable portion of worldwide energy consumption and subsequent carbon emissions, buildings, particularly their heating load (HL) and cooling load (CL), have emerged as key elements in the quest for substantial energy savings and a means of achieving a significant reduction in greenhouse gas emissions [2]. Despite the growing volume of data being generated that highlights potential advancements in energy management, a significant disparity between anticipated and actual building energy consumption remains [1, 3]. With an ever-diminishing store of energy resources and the escalating environmental repercussions, residential energy consumption has garnered significant attention from various sectors of society [4]. In this regard, ensuring efficient energy use in buildings, particularly concerning HL and CL, has become paramount. The increasing urgency stemming from depleting energy resources and growing environmental impacts has put residential energy consumption in the spotlight [5]. The

profound impact of a building's geographical location on temperature differences, a significant factor affecting heating and cooling loads, highlights the need for a more comprehensive understanding of influential parameters affecting the development of more energy-efficient buildings [6].

The importance of understanding and reducing HL and CL cannot be understated. These elements significantly influence overall building energy consumption. Despite the unwavering efforts of researchers in this field, a robust solution to managing and minimizing these loads effectively remains crucial [7]. The geographical location of a building profoundly impacts the temperature difference, a key variable affecting these loads [8]. While architects and engineers often seize on these limitations, a comprehensive understanding of other influential parameters can facilitate the design of more energy-efficient buildings. An extensive range of literature explores diverse facets of building design to optimize energy consumption. Investigations into various roof designs and materials, such as integrating hollow-core masonry and precast concrete slabs into buildings, have offered valuable insights [9, 10]. Nevertheless, a consistent issue that emerges in these studies is the challenge of multicollinearity or the excess dimensionality in building energy performance modeling. This issue indicates the necessity of a more refined approach towards constructing robust models in this area, emphasizing not only accuracy but also sensitivity issues to ensure reliable predictions and conclusions [11]. The global outlook of energy consumption underscores the urgency of this endeavor. Buildings account for a significant portion of world energy use, contributing to approximately 40% of all energy usage and 33% of CO2 emissions globally [11]. The imperative for energy-efficient building design is not just about conserving energy; building energy efficiency plays a crucial role in mitigating climate change by reducing greenhouse gas emissions. With the increasing interest in building energy load, optimizing these burdens emerges as an evident and effective strategy for substantial energy savings and reduced emissions [12].

However, traditional engineering-based building energy modeling often falls short and is unable to accurately predict actual energy usage due to various unpredictable factors, including occupancy patterns and weather fluctuations. This divergence from predicted to actual energy consumption highlights the pressing need for innovative approaches in building energy management [13, 14]. One such promising avenue is the integration of machine learning (ML), artificial intelligence (AI), and data-driven approaches in building energy management. The explosion of data generated by buildings, amplified by the Internet of Things (IoT), has cleared the way for a more complex and accurate approach to managing building energy consumption and other applications. Predictive algorithms, supported by historical energy consumption data and weather forecasts, hold the potential to revolutionize building energy management [15, 16]. These algorithms can empower building operators to make more informed decisions, optimizing energy use, and reducing costs. This newfound reliance on data goes beyond mere energy consumption estimating. Algorithms utilizing energy consumption data have aided the creation of regional energy-consumption maps, offering policymakers valuable insights for the efficient allocation of energy. This data-driven approach extends to the benchmarking of building stocks, allowing for a more streamlined and automated process and fostering a more informed and effective strategy for global retrofitting and improvements in building energy efficiency [17].

This data-driven method also facilitates the benchmarking of building stocks, enabling a more simplified and automated process. This enhancement contributes to a more informed and effective global strategy for retrofitting and enhancing building energy efficiencies. Hence, advancing energy performance efficiency in residential buildings is a multifaceted challenge that necessitates a fresh perspective and innovative approach. The integration of ML and explainable AI is a promising avenue, offering enhanced accuracy in energy consumption prediction and more informed decision-making processes, ultimately leading to substantial energy savings, emission reduction, and progress towards sustainable and energy-efficient residential buildings. This study is mainly aimed at contributing to the enhancement of residential buildings' energy efficiency by leveraging advanced computational techniques, specifically applying various ML models and ensuring their alignment with global sustainability visions such as the United Nations' Sustainable Development Goals (SDGs). For this purpose, the study drives the primary objective to enhance the energy efficiency of residential buildings by leveraging advanced computational techniques. Specifically, through comparative analysis, the study explores the performance of several ML models, including emotional neural learning (ENN), Gaussian process regression (GPR), and boosted tree (BT) algorithm in determining HL and CL. The study employed a dataset of 768 buildings that feature various engineering methods; the research is aimed at validating and assessing the reliability of these models through performance metrics. However, the key focus is placed on the effectiveness of the standalone models. Furthermore, by integrating explainable AI (AIX), the study ensures that the insights derived are accurate, interpretable, and actionable for stakeholders, highlighting the potential of these models in promoting sustainable building designs aligned with global sustainability visions.

2. State-of-the-Art Research

The recent state-of-the-art literature features a significant shift towards leveraging AI-based models in enhancing residential building energy efficiency modeling. Cutting-edge studies indicate AI's ability to accurately predict and optimize building energy consumption, surpassing traditional methodologies substantially. Advanced AI algorithms, particularly ML and deep learning models, have demonstrated exceptional adeptness in handling the complex nature of energy data, uncovering intricate patterns and relationships that are hard to discern using conventional analytical techniques. These innovative, AI-driven models aid the production of more precise, reliable, and immediate energy performance predictions, contributing to the design of

highly energy-efficient residential buildings. The use of AI in this context signals a transformation, indicating a new era of elevated energy efficiency, sustainability, and environmental stewardship in residential building design and operation. Various AI and ML models have been applied in computational analysis and prediction of building efficiency in terms of HL and Cl, such as artificial neural network (ANN), support vector regression (SVR), and linear and polynomial least square regression (PLS) [8, 18, 19]. For instance, Zhang and Haghighat [20] developed a regression approach to predict monthly heating demand for single-family homes in temperate climates. Aimed at assisting architects and design engineers in early project stages, the models facilitate swift parametric studies for optimizing building structures against various criteria. Cheng and Cao [7] introduced multivariate adaptive regression splines (MARS) for predicting building energy performance efficiently. MARS, combined with an artificial bee colony, optimizes parameter settings for minimal error. The results found were reliable according to their error values.

Similarly, Nilashi et al. [21] utilized AI-based models to devise an effective strategy to estimate household energy efficiency by employing ANN and SVR. However, their research overlooked hyperparameters' impact on their models' efficiency. Sekhar Roy et al. [22] explored ML methods to predict residential building energy consumption. They found that tree predictions were most effective with random forest (RF) or KNN but ignored the role of hyperparameters. In 2018, Dan and Phuc [23] investigated the utility of novel ML in predicting energy consumption for building designs. They scrutinized diverse ML algorithms without exploring the influence of parameter adjustments on performance results. Likewise, Li et al. proposed a cooling load prediction study using several ML models, viz., SVR and ANN, with SVR outperforming the ANN model. Similarly, other published literature proved the application of ML in building sectors [24, 25]. Furthermore, Jain et al. [26] highlighted the urgent need for advanced energy consumption forecasting in buildings. The study introduces a sensor-based SVR model that was used to analyze a New York residential building's data. The study identified optimal forecasting with hourly, by-floor monitoring, contributing significantly to future energy efficiency initiatives and smart metering deployment. A detailed application of ML in energy systems has been conducted by Entezari et al. [27]. Figure 1 displays the bibliographic information of a decade's review of AI and ML models used in an energy system. This analysis maps the recurrent keywords in various areas of an energy system. Figure 1 demonstrates the interconnected fields of AI and ML within the energy field, forming four major research clusters.

Notwithstanding numerous attempts and progress in the field, there remains a notable and unaddressed gap in the development of an ideal model utilizing a field of algorithms for increasing the accuracy of energy prediction [28]. Past efforts, such as the research conducted by [27, 29–31], have made meaningful contributions by examining the influence of various factors on the heating and cooling loads (HL and CL) in residential buildings. Their insights, particularly

regarding the significant impact of wall area and window-to-wall ratio, have shed light on the intricate dynamics of building energy consumption. Nonetheless, exploration of the scope of ML for energy forecasting has encountered substantial challenges. Addressing these difficulties, [32, 33] introduced a pioneering standalone and hybrid model. Their innovative approach, which combines improved optimization with a cutting-edge deep learning method, showcased exemplary performance, outshining alternative predictive methods in estimating both HL and CL. Yet, despite these advancements, the sector remains in its nascency, with a limited number of studies employing explainable ML to estimate building energy usage. In light of this, the present research employed a novel approach, aiming to enrich this growing field of study. It introduces a predictive model for building energy consumption, utilizing GPR, BT, and ENN models to consider both HL and CL. Subsequently, the outcome was integrated with the newly explainable ML approach based on SHapley Additive exPlanations (SHAP). This groundbreaking model fills a knowledge gap, offering an optimized configuration that substantially enhances energy consumption prediction using a combination of ML and advanced metaheuristic search-based techniques.

It is worth noting that the model's unique design and functionality are indicative of its potential to significantly reduce search complexity and elevate the precision of energy consumption predictions [34, 35]. This enhancement is not merely incremental but marks a substantial increase forward in the field of energy prediction. By accurately predicting building energy demands, this inventive model stands as a beacon in the mission to curtail energy wastage and augment energy efficiency in buildings [36]. This is not just a theoretical advantage; it translates into tangible benefits, including a reduction in energy costs and the expansion of access to cost-effective and clean energy [37]. Moreover, by incorporating AI-based model approaches, the model lays the foundation for a substantial increase in building energy efficiency, contributing to a marked reduction in the overall carbon footprint. This is essential in facilitating the global shift towards more sustainable and environmentally friendly energy sources, addressing not only the immediate concerns around energy efficiency but also the broader, more encompassing issue of global sustainability.

3. Methodology of Research

3.1. Data Background. To conform standard mathematical notation, the energy performance data for various building shapes were determined based on simulations using *Ecotect software*, as outlined in the research conducted by Tsanas and Xifara [38]. The dataset comprises information for 12 different building shapes, incorporating a total of 10 variables that include eight input and two output variables. The input variables comprise factors such as relative compactness (RC), surface area (SA), wall area (WA), overall height (OH), orientation (OT), glazing area (GA), and glazing area distribution (GD). The output variables include heating load (HL) and cooling load (CL). The orientation input variable contains four discrete values representing
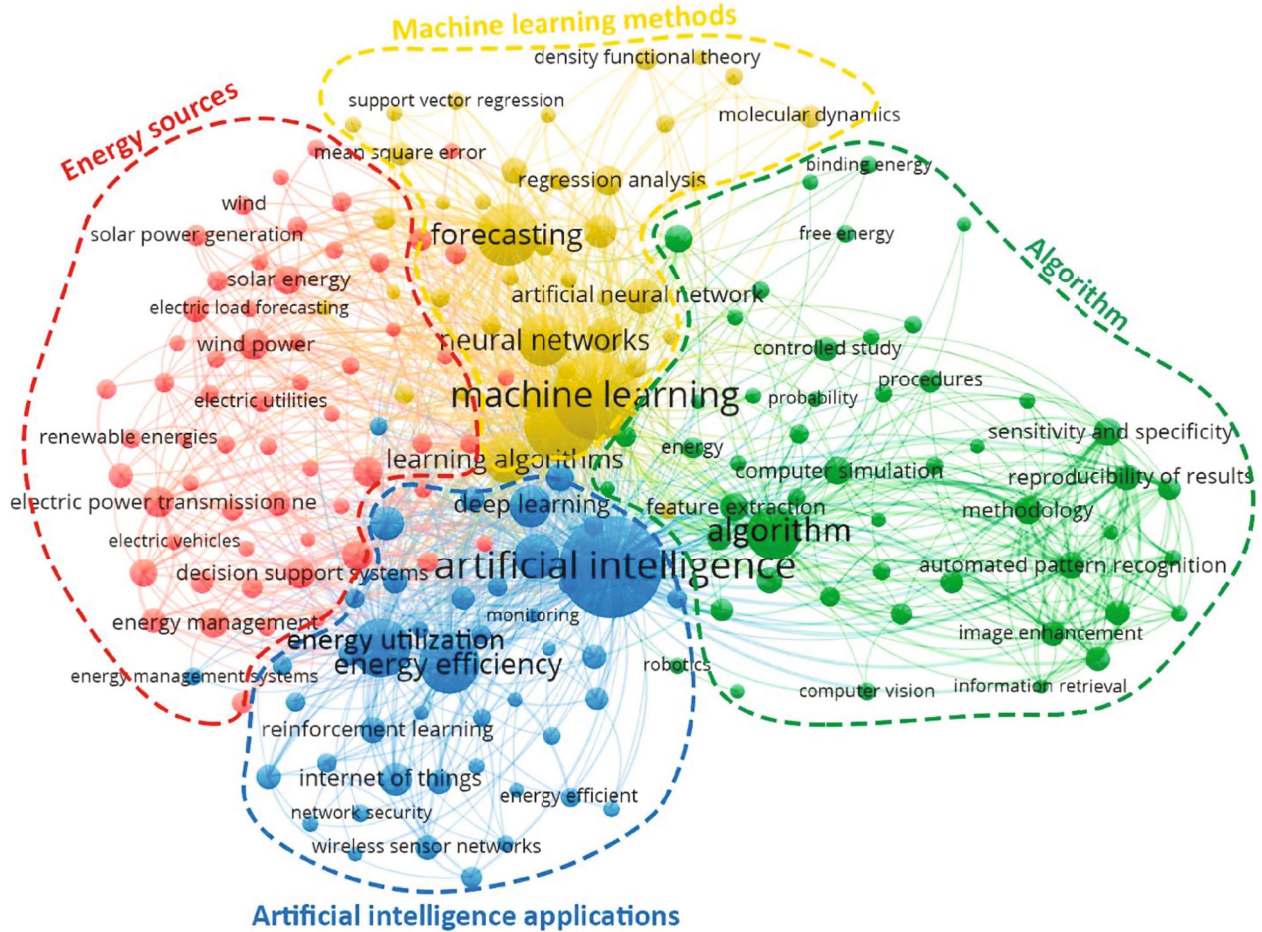
FIGURE 1: A comprehensive network of energy, AI, and ML models [27].

the cardinal directions, while the glazing area input variable consists of four discrete values representing various percentages of the floor area (0%, 10%, 25%, and 40%). Glazing area distribution is described by five discrete values corresponding to different distribution scenarios. A total of 768 simulated building cases are encompassed in this dataset, each characterized by the eight aforementioned input variables and the recorded HL and CL. For the simulated buildings, consistent volume (771.75 m^3), materials, and internal conditions are maintained to ensure uniformity in the simulations. The buildings, situated hypothetically in Athens, Greece, assume residential usage with specific internal design conditions that include clothing level, humidity, air speed, and lighting level. Various glazing area percentages and distributions, alongside different orientations, are used to simulate diverse building samples. Despite potential biases or inconsistencies in the simulation data, the experimental results are regarded as a reliable representation of actual real-world data for the purpose of this study, providing valuable insights into the likely changes and trends in the energy performance of buildings with varying parameters [21, 38, 39]. The standard serves as a basis for conducting and analyzing building energy performance simulations, facilitating energy comparisons of buildings, and contributing to the development of energy-efficient building designs.

3.2. Data Exploration and Building Information. The data source and quality were clearly stated by Tsanas and Xifara [38]; the potential biases or limitations in the dataset have already been addressed in [38]. This mathematical notation standard is based on the source dataset developed by Tsanas and Xifara [38], available in the UCI ML repository, which includes energy performance data from simulations of 12 distinct residential building types with a uniform volume of 771.75 m^3 but varying envelope features. The material selection for these buildings was meticulously chosen to achieve the lowest U-values, with specifications including walls at 1.78 m^{2}K/W, floors at 0.86, roofs at 0.50, and windows at 2.26. The window-to-floor ratio in the simulations varies from 0% to 40%, and six different glazing distribution scenarios, ranging from uniform glazing to no glazing, are applied. Each simulated building is occupied by seven individuals predominantly involved in sedentary activities. The ventilation system operates in mixed mode with a 95% efficiency and a thermostat setpoint range of 19–24°C. The operational hours for the buildings are set from 3 pm to 8 pm (15:00–20:00) on weekdays and from 10 am to 3 pm (10:00–15:00) on weekends. Furthermore, a consistent lighting level of 300 lux is maintained in all building simulations. Despite the simulated nature of the data, it offers

RC = 0.98   RC = 0.90   RC = 0.86   RC = 0.82

RC = 0.79   RC = 0.76   RC = 0.74   RC = 0.714

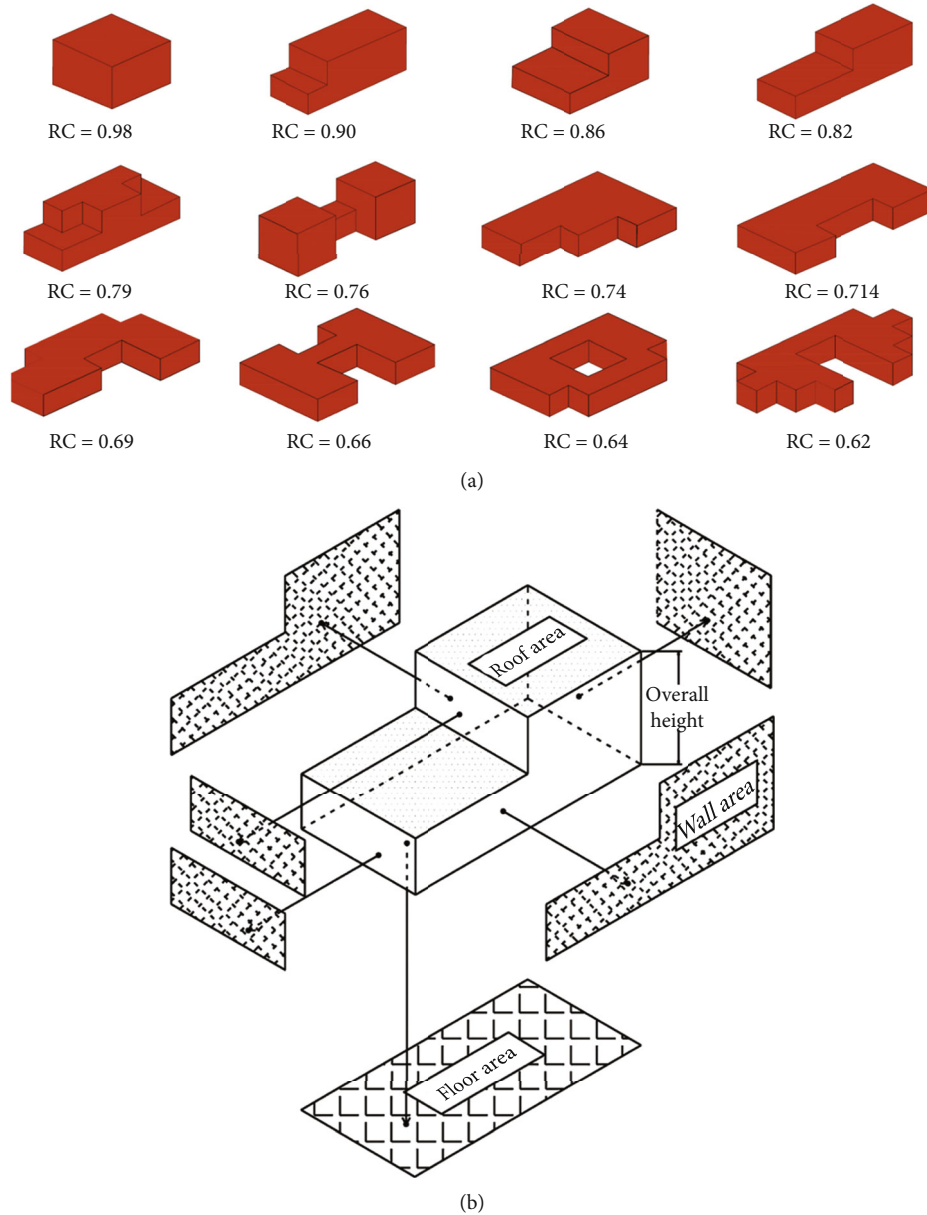RC = 0.69   RC = 0.66   RC = 0.64   RC = 0.62

(a)

(b)

FIGURE 2: (a) Building shape and (b) genetic definition of building areas.

substantial insights into the energy performance of various building types, aiding in the assessment and comparison of energy efficiency across diverse building designs and parameters (see Figure 2(a)). The selected materials for the simulation had the lowest contemporary U-values, with specific values for walls, floors, roofs, and windows. The internal conditions of the buildings were also meticulously set, including factors like clothing, humidity, air speed, and lighting level. The simulation used a mixed mode with 95% efficiency and a thermostat range of 19–24°C. Operational times were assigned as 15–20 hours on weekdays and 10–20 hours on weekends (see Figure 2(b)). Further details about the simulations are provided in the study by Baalousha [40]. The number of cases and a visual representation are presented in Table 1.

TABLE 1: Input-output variables and representations.

Abbreviation	Target variable	No. of possible values
RC	Relative compactness	12
SA	Surface area	12
WA	Wall area	7
RA	Roof area	4
OH	Overall height	2
OT	Orientation	4
GA	Glazing area	4
CG	Glazing area distribution	6
HL	Heating load	586
CL	Cooling load	636

3.3. Data Processing, Reliability, and Analysis. Generally, data processing, reliability, and analysis are critical elements for extracting meaningful insights from raw data. Efficient data processing entails collecting, cleaning, and transforming raw data into a usable format and thus ensuring its reliability for analysis [41]. Reliability highlights the consistency and stability of data, which is fundamental for accurate analysis and decision-making. It ensures that the data accurately represent the information they are intended to measure and are free from errors and biases. Table 2 outlines the statistical characteristics of the utilized datasets. Figure 3 graphically demonstrates the distribution of data parameters engaged in formulating the model. These visual interpretations are essential in identifying variable values lacking sufficient data, highlighting areas necessitating additional data for enhancing the model's predictive accuracy [42]. In this paper, the computations reported are for both data preprocessing and postprocessing and are integral. This necessity primarily stems from the requirement for outlines, and the cleaning process was conducted as mentioned in the results section (Figure 3). This process is vital as it represents the covariance information among variables, supporting the accurate depiction of dependencies. However, all variables in the study were normalized prior to the model development, ensuring a mean of zero and a variance of one, as achieved by a specific linear transformation (Eq. (1)). This approach accounts for each of the eight input and two output variables used in the study, each represented with a specific index and transformed accordingly. The means, standard deviations, minimum, and maximum values of each variable, calculated from dataset samples, are presented for reference (see Table 2). Estimations and predictions from the models are reconverted to their original values using an inverse transform to ensure clarity and consistency in data interpretation [43–46].

$$y = 0.05 + \left(0.95\left(\frac{x - \bar{x}}{x_{\max} + x_{\min}}\right)\right), \quad (1)$$

where y represents normalized data. x is the measured data, $\bar{x}$ is the mean of the measured data, $x_{\max}$ is the maximum value of the measured data, and $x_{\min}$ is the minimum value.

3.4. Model Validation and Performance Indicators. Model validation and performance indicators are crucial in assessing the effectiveness and reliability of predictive models [47–49]. In this context, a 10 k-fold cross-validation method is employed to ensure the robustness of the models, BT, NNN, and GPR, used in predicting outcomes (HL and CL). This technique helps in maximizing the utilization of available data by partitioning it into ten subsets, where the model is trained on nine subsets and iteratively validated on the remaining one (see Figure 4). Regarding performance indicators, RMSE (root mean square error) and MAE (mean absolute error) are used to quantify the deviation of the model predictions from actual values, providing insights into the model's accuracy. The Pearson coefficient of determination (PCC) offers a measure of how well the model's predictions match the observed data, wherein a value close

Table 2: Basic descriptive statistics of the study.

Variables	Mean	SD	Kurtosis	Skewness	Min	Max
RC	0.76	0.11	-0.71	0.50	0.62	0.98
SA	671.71	88.09	-1.06	-0.13	514.50	808.50
WA	318.50	43.63	0.12	0.53	245.00	416.50
RA	176.60	45.17	-1.78	-0.16	110.25	220.50
OH	5.25	1.75	-2.01	0.00	3.50	7.00
OT	3.50	1.12	-1.36	0.00	2.00	5.00
GA	0.23	0.13	-1.33	-0.06	0.00	0.40
GA	2.81	1.55	-1.15	-0.09	0.00	5.00
HL	22.31	10.09	-1.25	0.36	6.01	43.10
CL	24.59	9.51	-1.15	0.40	10.90	48.03

SD = standard deviation; Min = minimum; Max = maximum.

to 1 indicates a good fit. Additionally, MAPE (mean absolute percentage error) is used as an indicator to understand the relative error in predictions, thus offering a perspective on the model's performance in terms of percentage error. The combination of these robust validation techniques and comprehensive performance indicators facilitates an in-depth assessment of the BT, NNN, and GPR models, ensuring their reliability and effectiveness in predictions. The predictive model's performance was evaluated using various criteria (Table 3).

It is worth mentioning that evaluating model effectiveness entailed the utilization of a k-fold cross-validation technique [54]. This method significantly reduces the bias introduced by the random selection of test cases, enhancing the reliability of model assessment as highlighted by previous studies. Some researchers indicate that employing ten folds strikes an optimal balance between bias and variance, in addition to time efficiency, in the validation process [55]. In line with this, the current research implemented a stratified 10-fold cross-validation to ascertain the models' average performance effectiveness [56, 57]. By partitioning the randomly selected data into ten unique folds, each was used sequentially as a testing set, while the others served as a training set. This approach ensures the comprehensive application of all data instances in both training and testing stages, offering a more rounded and thorough model evaluation. The final measure of algorithm accuracy is articulated as the mean accuracy derived from the ten models across the ten validation rounds, providing a robust overview of the model's predictive capabilities and reliability in various scenarios.

3.5. Proposed AI-Based Methods. Over the past several decades, the implementation of computational methodologies in process engineering fields, notably in systems like energy, has witnessed a significant transformation and improvement. AI as a data-driven approach has several sources of acceptable data, including field investigation, experimental work, satellite data, sensor data, and online monitoring. The present research is aimed at establishing the interpretative and predictive powers of unique AI-based models, namely, GPR, BT, and NNN, with the final being recognized as a frequently utilized neural network.
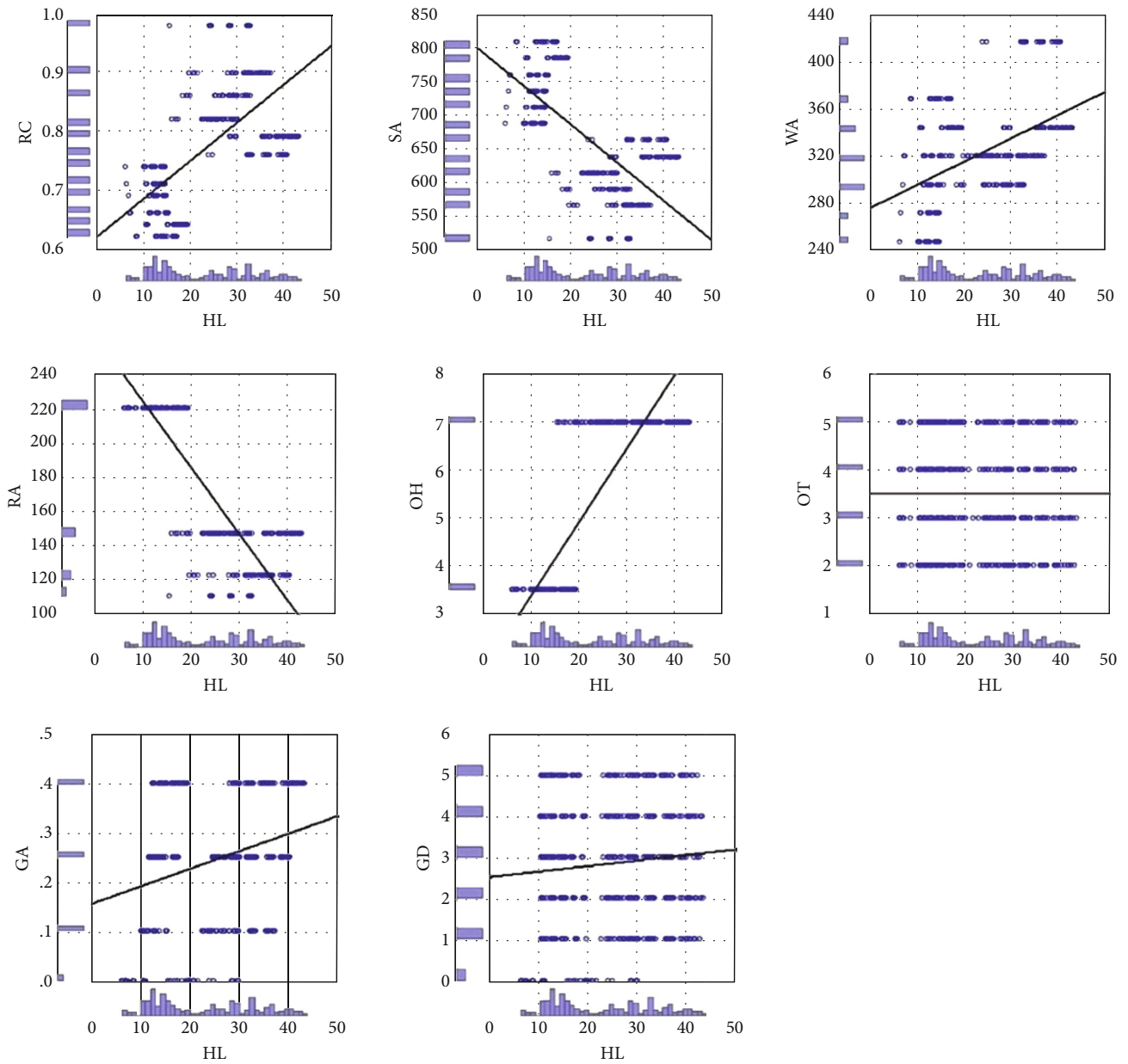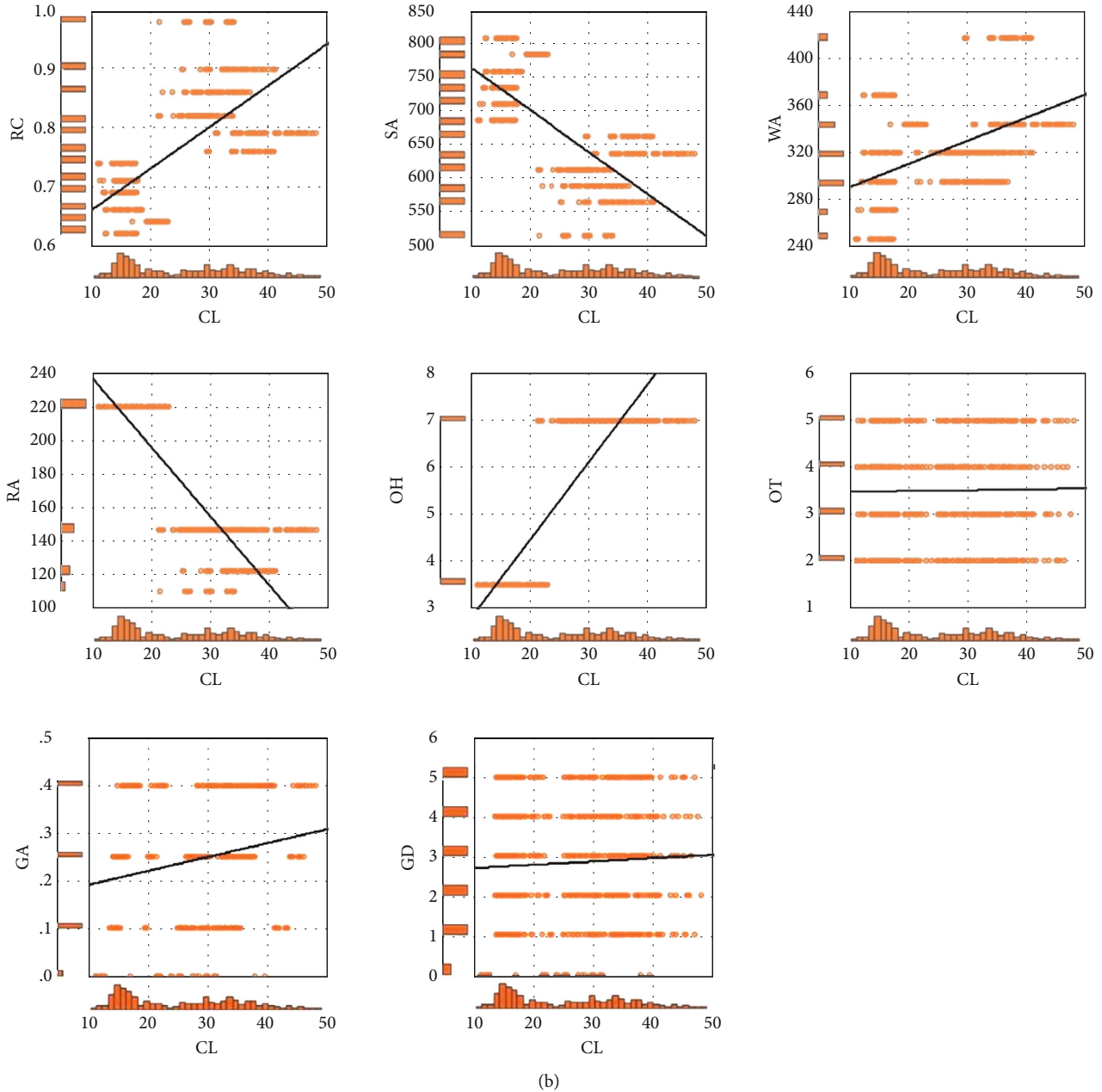
(a)

Figure 3: Continued.

(b)

Figure 3: Bivariate analysis of input and output variables: (a) HL and (b) CL.

These models are intended to aid in the modeling and parametric fine-tuning of energy efficiency within residential buildings. A necessary phase in creating such intelligence-laden, data-driven models is the thorough preprocessing of the collected data, followed by the appropriate selection of the most fitting model. Recognizing the inherent intricacy of these models, a multifaceted approach leveraging diverse AI models becomes imperative. This ensures a comprehensive understanding of the AI's capabilities, especially when tackling complex and naturally nonlinear processes that are characteristic of operations like energy systems. The summary of the proposed approach is presented in Figure 5 as a flowchart methodology. While the use of AI models in enhancing building energy efficiency offers signif-

icant advantages, it is important to consider potential challenges and limitations. Advanced AI models, like those involving ENN and GPR, are computationally intensive, requiring substantial processing power, which might not be economically feasible for all. The effectiveness of these models heavily depends on the quality and quantity of data, and gathering comprehensive, accurate data for numerous buildings is a massive and complex undertaking. Even with the integration of explainable AI (AIX), the interpretability of complex algorithms remains a challenge, especially for stakeholders without a technical background. Furthermore, the generalizability and scalability of these models to different building types and environments, their adaptation to real-time changes, and their integration with existing
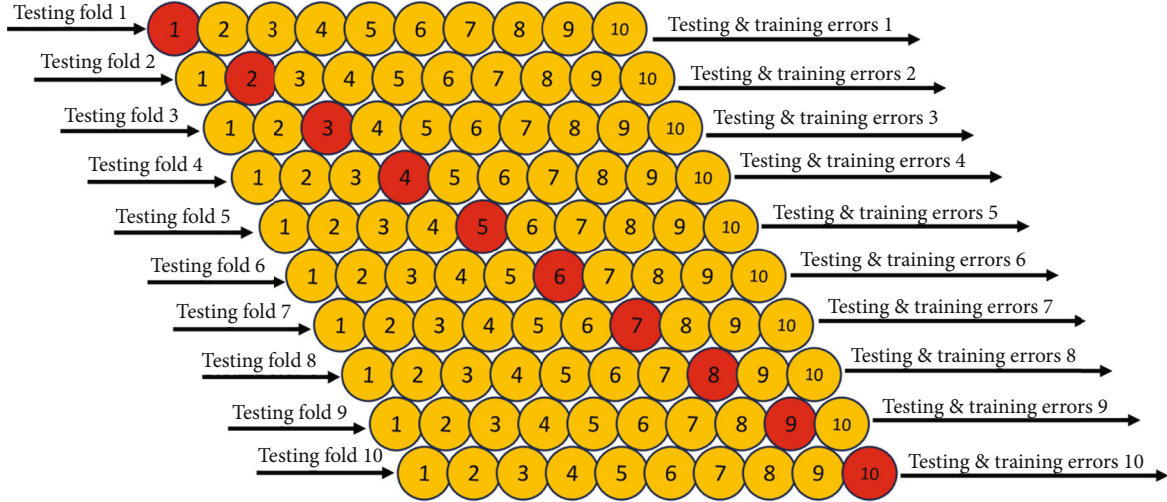
Figure 4: 10 k-fold cross-validation methods.

Table 3: Formulas of different performance measures.

Equation	Ranges	References
$PCC = \dfrac{\sum Y_0 - Y_{om}\left(Y_p - Y_{pm}\right)}{\sqrt{\left(Y_p - Y_{pm}\right)^2 - \left(Y_0 - Y_{0m}\right)^2}}$	$-1 < CC < 1$	[50]
$RMSE = \sqrt{\dfrac{1}{N}\sum_{i=1}^{N}\left(Y_{(p)} - Y_{(o)}\right)^2}$	$0 < RMSE < \infty$	[51]
$MAE = \dfrac{\sum_{i=1}^{N}\left|Y_{(p)} - Y_{(o)}\right|}{N}$	$0 < MAE < \infty$	[52, 53]
$MAPE = \dfrac{100}{N}\sum_{I=1}^{N}\left|\dfrac{Y_{(O)} - Y_{(P)}}{Y_{(o)}}\right|$	$0 < MAPE < 100$	[51]

building systems can be complex and costly. Moreover, the long-term reliability and maintenance of these AI systems, considering the rapid evolution of AI technologies, and the significant upfront costs associated with implementing such solutions present further obstacles. These challenges underscore the need for careful consideration and strategic planning in the deployment of AI for building energy efficiency.

3.6. Theory of Predictive Models. In this section, we explore the standalone AI-based techniques for accurate estimation and parametric optimization of energy consumption patterns in terms of HL and CL. The selection of these specific techniques was carefully done, taking into account their robust ability to predict complex systems such as energy systems in science and engineering. In this work, we want to explain the main ideas, how we use them, and why we chose these AI-based methods. The main goal is to make it easy to understand the proposed approach and show that the prediction model is flexible and strong.

3.6.1. Gaussian Process Regression (GPR). Gaussian process regression (GPR), also known as Kriging, is a Bayesian, nonparametric approach to regression that directly infers a dis-

tribution over functions, rather than just function parameters [58] (see Figure 6(a)). At its core, GPR uses a mean function to represent average behavior and a covariance function (or kernel) to determine how correlated data points are. This allows GPR to provide not only a predicted output for a given input but also a measure of prediction uncertainty. While it excels in modeling nonlinear relationships and estimating uncertainty, GPR can be computationally demanding for large datasets and requires careful kernel selection [59]. It is widely used in areas like geostatistics and ML, where prediction uncertainty is paramount [60]. The following is the general expression of the GPR model that links the explanatory vector (x) and the response (y):

$$y_i = f(x_i) + \varepsilon. \tag{2}$$

The function $f(x)$ for any unobserved pair (x^*, f^*) in which f is the response and x is the explanatory parameters obtained by

$$\begin{bmatrix} f \\ f^* \end{bmatrix} \sim Nn + 1\left(0, \begin{bmatrix} K(X,X) & k(X,x^*) \\ k(x^*,X) & k(x^*,x^*) \end{bmatrix}\right). \tag{3}$$
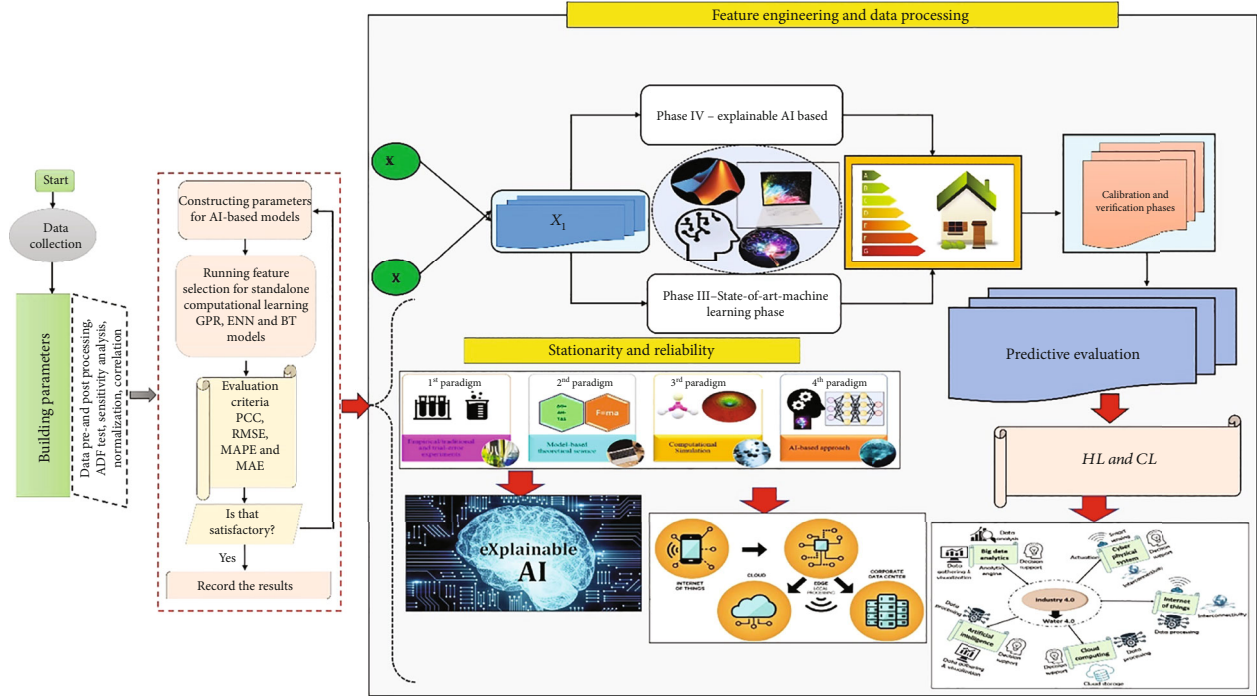
FIGURE 5: Proposed flowchart used in this study.

In Eq. (3), $K(X, X)$ represents the matrix of covariances $(n \times n)$ for all samples in the calibration data.

3.6.2. Boosted Trees (BT).

BT is a supervised ML method used for both classification and regression. They split data based on feature values, forming tree-like models of decisions (see Figure 6(b)). Each node represents a feature, each branch a decision rule, and each leaf a result [61]. They are intuitive and easy to visualize but can be prone to overfitting if not pruned. BT structure complex solutions in a tree-like structure by dissecting those solutions into smaller, more manageable possibilities. To offer precise class assignments, decision trees use splits to select attributes that minimize entropy [62]. It is simpler to grasp the model because of its visual representation and significant insights. While ensembles like random forests and boosting increase prediction accuracy, pruning strategies reduce overfitting [63].

$$f(x) = \begin{cases} c_1 \text{ if } x_i \le T_i \\ c_2 \text{ if } x_i > T_i \end{cases}. \qquad (4)$$

$f(x)$ is the prediction made by the decision tree.
X_i is the ith feature.
T_i is the threshold for the ith feature.
c_1 and c_2 are the predicted classes or values for the corresponding branches.

3.6.3. Emotional Neural Network (ENN).

Emotional neural networks (ENN) integrate emotion modeling into traditional neural networks, enhancing machines' capability to recognize or simulate human emotions [64]. By analyzing data patterns, like facial expressions or voice modulations, ENNs can infer underlying emotions such as joy, sadness, or anger [65]. This is crucial in human-computer interactions, especially in areas like virtual assistants, therapy bots, or gaming (see Figure 6(c)). The goal is to make interactions more natural and responsive to human feelings. However, achieving accurate emotion recognition remains challenging due to the complexity and subjectivity of emotions. With further research, ENNs hold the potential to bridge the emotional gap between humans and machines [66–69]. It is possible to calculate the output of the ith neuron in an EANN with three hormonal glands, H_a, H_b, and H_c.

$$Y_i = \left(\gamma_i + \sum_h \partial_{i,h} H_h \right) \times f \left(\sum_j \left\lfloor \left(\beta_i + \sum_h X_{i,h} H_h \right) \right. \right.$$
$$\left. \left. \times \left(\left(\propto_{i,j} + \sum_h \Phi_{i.j.k} H_h \right) X_{i,j} \right) + \left(\mu_i + \sum_h \Psi_{i,h} H_h \right) \right\rfloor \right). \qquad (5)$$

The artificial hormones are calculated as

$$H_h = \sum_i H_{i,h} (h = a, b, c). \qquad (6)$$

The weight implemented for goal (f) in Eq. (5) is represented by (4).

4. Result and Discussion

The selection of these specific variables is underpinned by their substantial impact on the energy efficiency of
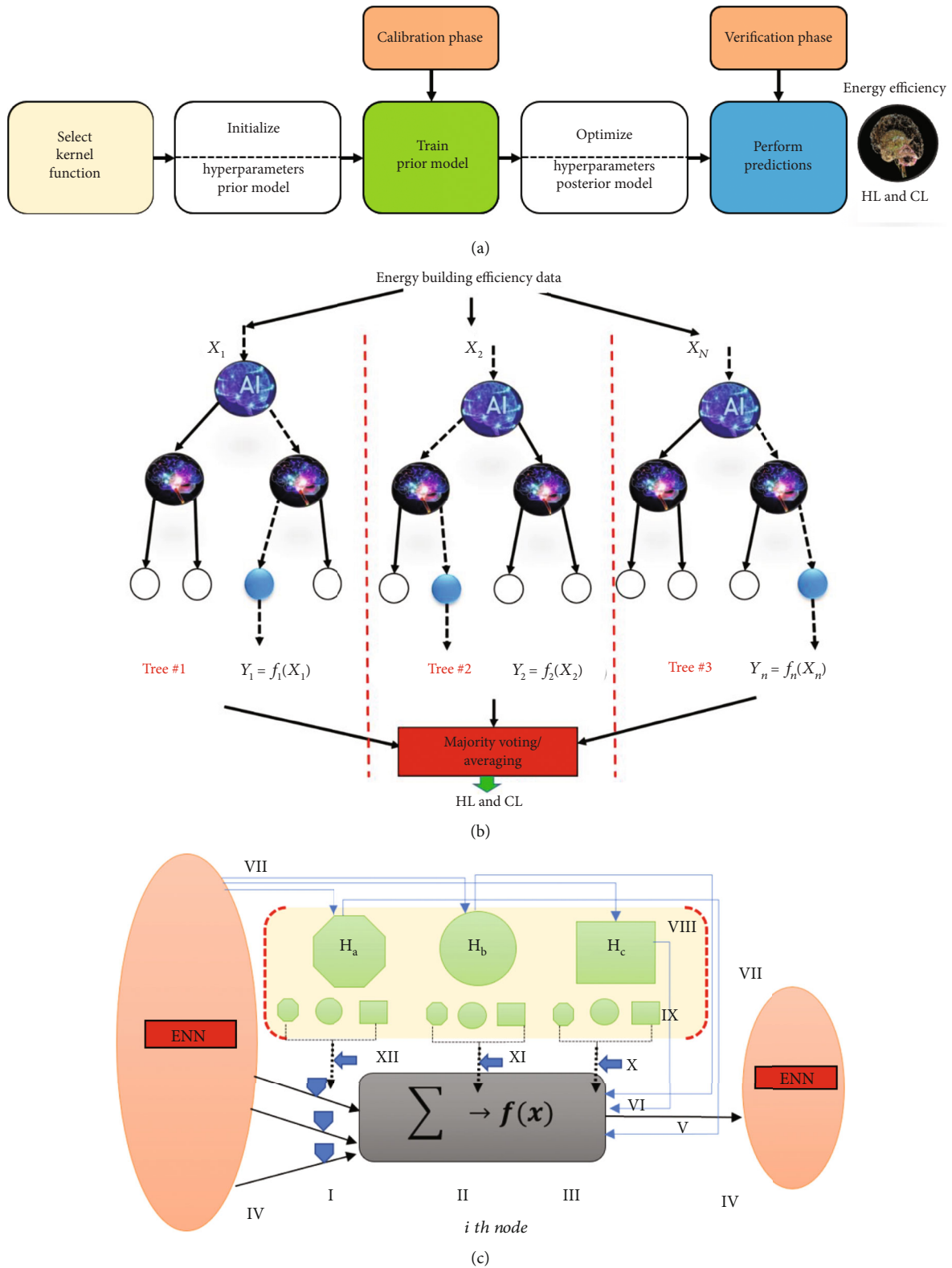
(a)

(b)

(c)

Figure 6: Structure and flow diagram of (a) GPR, (b) BT, and (c) ENN models.

residential buildings. This significant influence was highlighted in a study by Tsanas and Xifara, illustrating the potential of employing these variables for accurately determining a building's energy efficiency using statistical ML tools. Further, these variables have been utilized in an artificial neural network model for estimating the energy performance of structures, which reinforces their relevance in this context. Elements like surface area (SA), wall area (WA),
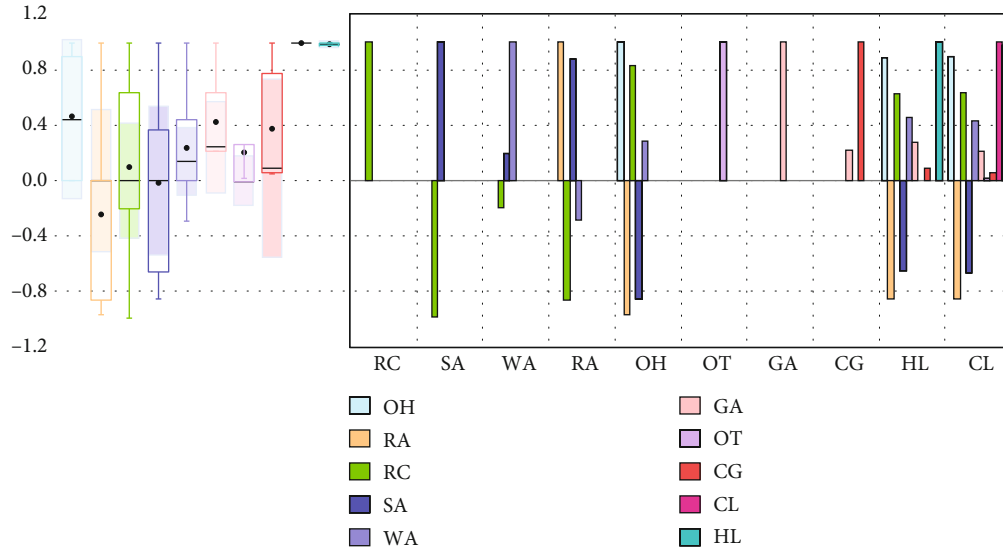
Figure 7: Input variable and linear feature engineering selection.

Table 4: Performance results for heating-loading-based building energy efficiency.

Models	Calibration phase				Verification phase			
	PCC	RMSE	MAE	MAPE	PCC	RMSE	MAE	MAPE
GPR-M1	0.9070	4.2965	3.2496	18.1679	0.9506	4.5779	3.4299	13.0575
GPR-M2	0.9614	2.9780	1.9147	11.7599	0.9976	3.2217	3.0424	12.8812
GPR-M3	0.9990	0.4248	0.2985	1.3844	0.9988	0.5146	0.3874	1.7141
BT-M1	0.9070	4.2963	3.2598	18.2225	0.9504	4.5793	3.4250	13.0215
BT-M2	0.9614	2.6885	1.8149	10.7575	0.9975	4.2097	3.9763	16.5940
BT-M3	0.9970	1.2076	0.9152	4.1517	0.9983	1.5621	1.3544	5.4528
ENN-M1	0.8947	4.5347	3.5025	19.1457	0.9419	4.7858	3.5531	13.3336
ENN-M2	0.9600	3.0230	2.0185	12.6051	0.9962	3.2665	3.0427	12.8040
ENN-M3	0.9865	1.5874	1.2416	6.9545	0.9919	1.3286	1.0056	4.3299

roof area (RA), and overall height (OH) are integral components of the building envelope. This envelope acts as a crucial physical separator between the indoor and outdoor spaces of a building, directly affecting its energy efficiency. Additionally, a building's orientation (OT) plays a pivotal role in regulating the amount of solar radiation it receives. Similarly, the glazing area (GA) and glazing distribution (GD) significantly influence the levels of natural light and solar radiation penetration into the building. Collectively, these factors underscore the critical role that these variables play in enhancing the predictive accuracy of ML models for estimating residential building energy loads, as corroborated by previous research. It is important to note that for the development of the GPR and BT model, MATLAB (2022b) was used for the analysis while MATLAB (2017) was applied for the ENN model. The graphical visualization was done using Eviews-10 and R-studio software.

The input combinations C1 (OH, RA), C2 (OH, RA, RC, and SA), and C3 (OH, RA, RC, SA, WA, and GA) were used based on feature engineering techniques. From Figure 7, the output's HL behavior can be understood in relation to other variables. There is a positive moderate correlation with RC

(0.6223), indicating a tendency for HL to increase as RC increases. On the other hand, HL decreases as SA rises, as is highlighted by their negative moderate correlation (-0.6581). The strong negative correlation with RA (-0.8618) suggests a pronounced decrease in HL when RA increases. However, a strong positive correlation (0.8894) with OH suggests the opposite; HL tends to significantly increase as OH increases. Other variables like OT show minimal impact on HL. It is also notable that HL and CL have a very strong positive correlation of 0.9759, which is not surprising. Similarly, examining CL's relationship with other variables reveals insights into its behavior. A moderate positive correlation with RC (0.6343) implies that CL generally increases with RC. On the other hand, SA's rise likely leads to a decrease in CL, as suggested by a negative moderate correlation (-0.6730). Strong negative (-0.8625) and positive (0.8958) correlations with RA and OH, respectively, indicate the significant influence that those variables have on CL. Most other variables have a weaker, though still noteworthy, impact on CL. However, due to the low correlation of OT and GA with corresponding target variables HL and CL of less than 27%, we decided to drop them from the modeling
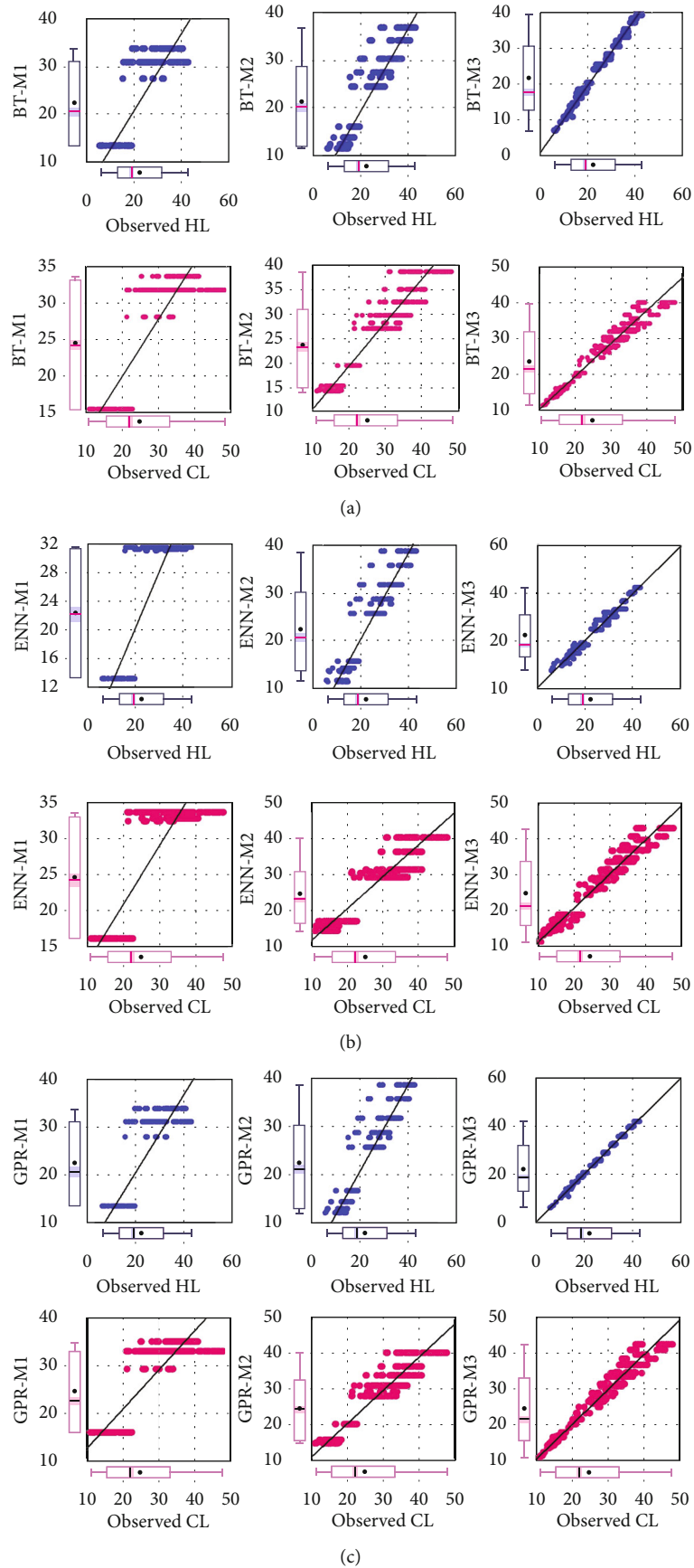
FIGURE 8: Scatter plots showing the predicted and measured values for (a) BT, (b) ENN, and (c) GPR.

TABLE 5: Performance results for cooling loading-based building energy efficiency.

	Calibration phase				Verification phase			
	PCC	RMSE	MAE	MAPE	PCC	RMSE	MAE	MAPE
GPR-M1	0.9122	3.9170	2.9586	13.0233	0.9373	4.1717	3.0187	10.3308
GPR-M2	0.9669	2.5534	1.8331	7.9534	0.9839	2.9060	2.4337	9.1846
GPR-M3	0.9858	1.5537	0.9807	3.4820	0.9856	1.6620	1.1200	3.7157
BT-M1	0.9122	3.7921	2.7099	11.2299	0.9373	4.8755	3.6608	12.8637
BT-M2	0.9669	2.3698	1.7078	6.9924	0.9839	3.8342	3.3110	12.6301
BT-M3	0.9840	1.9502	1.3287	4.9661	0.9853	2.2219	1.6184	5.7117
ENN-M1	0.8993	4.1653	3.1975	13.8809	0.9306	4.3302	3.0965	10.4926
ENN-M2	0.9486	3.0834	2.4555	11.1264	0.9730	3.2273	2.5407	9.2624
ENN-M3	0.9766	1.9914	1.5204	6.6260	0.9791	2.0030	1.5801	6.1763

schema in order to reduce the complexity of the input variables [70–72]. Table 4 indicates the predictive performance of HL using several AI-based models.

However, enhancing the generalizability of ML models requires hyperparameter optimization, a critical step in training ML algorithms. This ensures that models do not overfit or underfit and maintain minimal complexity. Using methods like GPR, BR, and ENN can improve the model's accuracy, efficiency, and performance. This optimization examines every combination of hyperparameters within their respective ranges to identify the best values. For GPR, the model of the hyperparameter is the kernel, with popular choices being the radial basis function (RBF); for instance, the RBF kernel has a length scale, typically in the range [0.1, 2.0], dictating the function's flexibility. Another vital hyperparameter is the noise level, often between [1e-3, 1e+3], which represents data noise and aids in fitting noisy observations. Some models may also incorporate regularization functions. For ENNs, hyperparameters often mirror those of standard neural networks. The learning rate is pivotal and can vary widely, typically within [1e-6, 1e-1]. Batch size, often between [16 and 512], dictates the number of samples processed before updating model weights. The number of epochs, usually in the range [10, 1000], represents full training dataset passes. Activation functions, like ReLU, sigmoid, or tanh, determine node outputs. Dropout rates, commonly set between [0, 0.5], are regularization techniques, with a higher rate dropping more neurons. The network's architecture, including the number of layers and units per layer, also plays a significant role.

In the assessment of HL-based building energy efficiency, the GPR-M3 model clearly excels during both calibration and verification phases, achieving the highest PCC at 0.9990 and the lowest values for RMSE, MAE, and MAPE, making it the most accurate among the GPR models. Similarly, BT-M3 surpasses its counterparts, BT-M1 and BT-M2, in all metrics during the calibration phase, indicating either a possibly optimized structure or refined parameters (see Figure 8(a)). Moreover, among the ENN models, ENN-M3 stands out with its notably lower MAPE of 6.9545 during the calibration phase. Although ENN models generally show a marginally reduced PCC in comparison to GPR and BT, their RMSE, MAE, and MAPE metrics remain

competitive, underscoring their reliable prediction capabilities (see Figure 8(b)). A consistent observation is the superior performance of the M3 variant across all model categories, possibly due to more advanced or meticulously adjusted hyperparameters. This underscores the paramount role of hyperparameter refinement and model optimization in heightening predictive accuracy in building energy efficiency tasks. Besides, in the numerical and in-depth analysis of the HL-based building energy efficiency models, the GPR-M3 model emerged as the most efficient. During the calibration phase, it recorded a PCC of 0.9990, outperforming GPR-M1 by 9.2% and GPR-M2 by 3.9%. It also boasted an RMSE value of 0.4248, a reduction of 90% and 85.7% compared to GPR-M1 and GPR-M2, respectively. This superior performance continued in the verification phase. Similarly, in the BT models, BT-M3 outshined the others with a PCC of 0.9970 and a significant reduction in RMSE values. ENN-M3 showcased a PCC of 0.9865, surpassing ENN-M1 by 10.3% and ENN-M2 by 2.8%. Its RMSE was also significantly lower. Conclusively, across all model types (GPR, BT, and ENN), the M3 variants demonstrated the highest precision, with GPR-M3 standing out due to its remarkably low RMSE values, underscoring its unmatched accuracy in predicting building energy efficiency across both phases.

Table 5 presents the predictive performance of CL in both the calibration and verification phases. In the calibration phase, GPR-M3 is superior, with the highest PCC at 0.9858, marking an 8.1% and 1.9% improvement over GPR-M1 and GPR-M2, respectively. It also achieves the lowest RMSE of 1.5537, a 60.3% and 39.2% reduction from GPR-M1 and GPR-M2. This trend extends to the verification phase, where GPR-M3 maintains the highest PCC (0.9856) and the lowest RMSE (1.6620). Similarly, BT-M3 outperforms in the calibration phase with a PCC of 0.9840, closely matching BT-M2 at 0.9669. Its RMSE stands at 1.9502, a 48.6% and 17.7% reduction from BT-M1 and BT-M2, respectively. In the verification phase, BT-M3 exhibits a PCC of 0.9853, a slight increase from its M1 and M2 counterparts, and an RMSE of 2.2219, showcasing its efficiency. ENN-M3 demonstrates excellence in the calibration phase, securing a PCC of 0.9766, 8.6% and 2.9% higher than ENN-M1 and ENN-M2. It also achieves a commendable RMSE of 1.9914, which is 52.2% and 35.4% less than
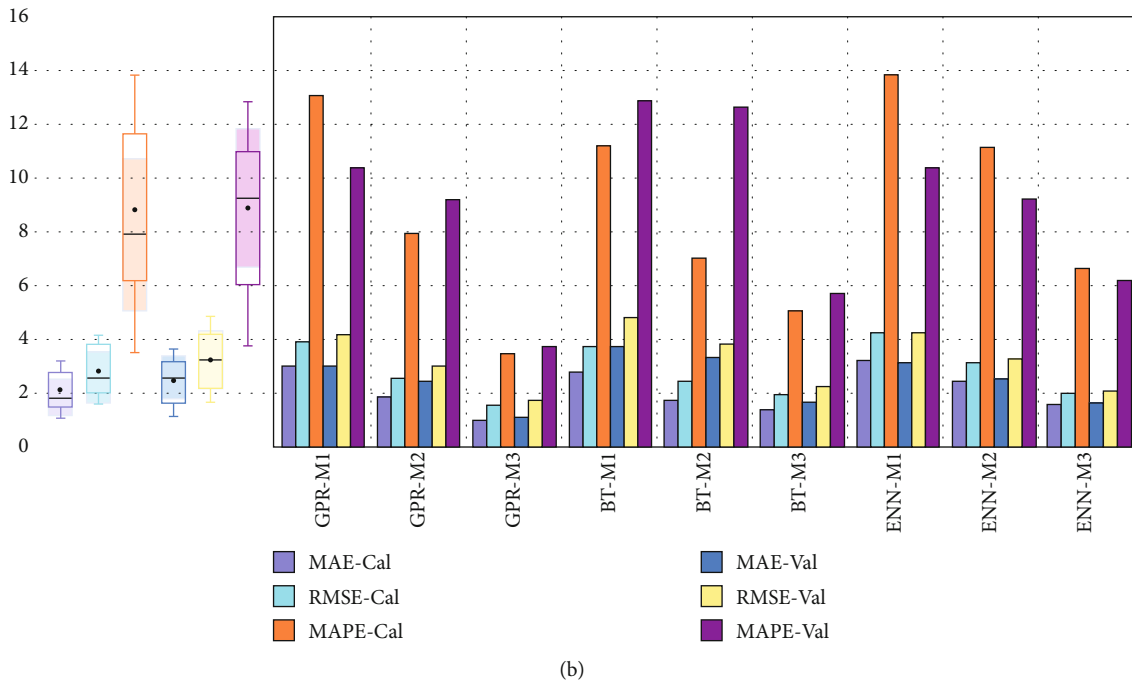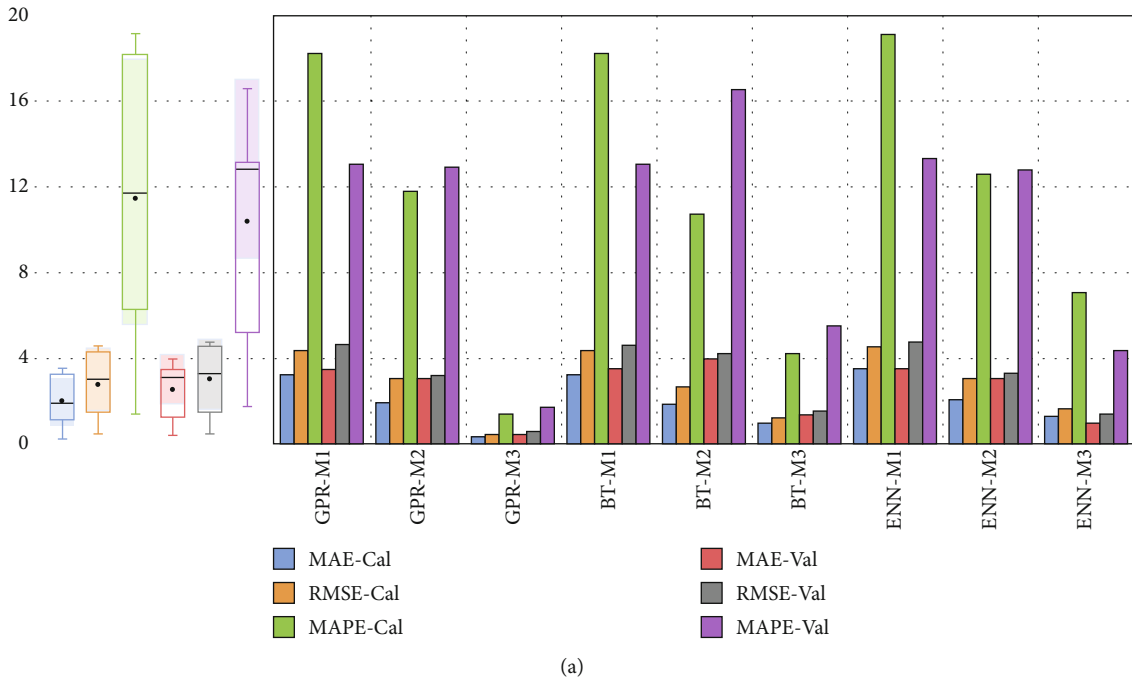
(a)

(b)

FIGURE 9: Error plot between the observed and predicted values: (a) HL and (b) CL.

ENN-M1 and ENN-M2, respectively. In the verification phase, ENN-M3's PCC reaches 0.9791, while its RMSE remains the lowest among the ENN models at 2.0030. Comparatively, the M3 variants across GPR, BT, and ENN consistently surpass their M1 and M2 counterparts in both the calibration and verification phases. It is worth mentioning that the GPR-M3 model distinguishes itself with its notably lower RMSE values, suggesting its enhanced precision in predicting CL-based building energy efficiency across both phases (see Figure 8(c)).

Numerical analysis of Table 3 focused on CL-based building energy efficiency, and the M3 models consistently display enhanced precision across all categories. Specifically, GPR-M3 in the calibration phase demonstrates a significant reduction in MAE (0.9807) and MAPE (3.4820%), outperforming its GPR counterparts by over 66% in MAE and 73% in MAPE. BT-M3 follows a similar trend, with its calibration phase MAE and MAPE values indicating a 50.9% and 55.7% reduction from BT-M1. In the ENN category, ENN-M3 outshines with a 63.5% and 52.3% decrease in
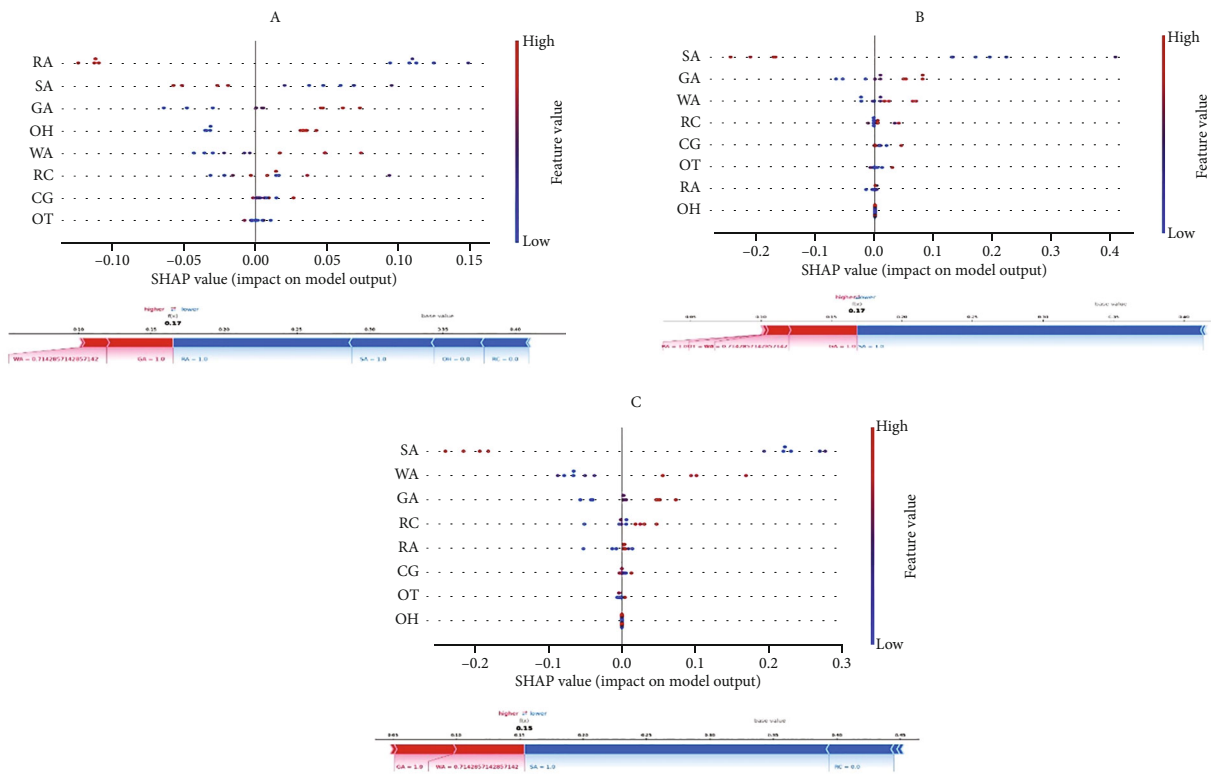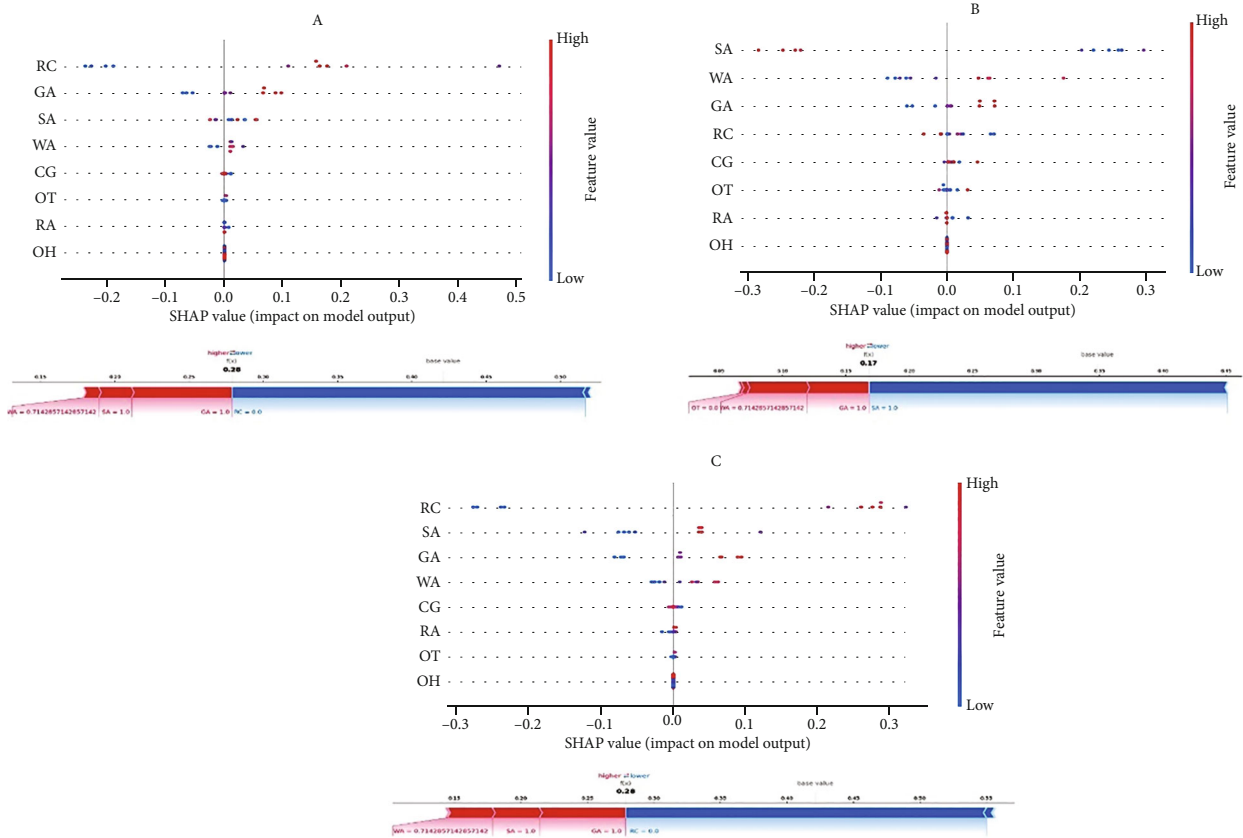
Figure 10: Summarized SHAP for (a) HL ((A) GPR, (B) BT, and (C) ENN) and (b) CL ((A) GPR, (B) BT, and (C) ENN models).

MAE and MAPE, respectively, compared to ENN-M1. During the verification phase, these M3 models maintain their lead, with GPR-M3 standing out with the lowest MAE (1.1200) and MAPE (3.7157%). Figure 9 shows the error plot of HL and CL based on error performance criteria. This underlines the superiority of the M3 model in predicting building energy efficiency with higher accuracy and precision. Through examination of the above results, which depict the performance metrics for HL- and CL-based building energy efficiency, it is evident that the M3 models, especially GPR-M3, consistently outshine their counterparts. Their unique precision suggests a significant potential for these models in real-world applications. Moving forward, it would be beneficial to delve deeper into the specific attributes of M3 models, expand datasets to encompass varied building structures, and incorporate features like occupancy patterns for enhanced prediction. Stakeholders should prioritize the adoption of these models, especially GPR-M3, and consider their integration into smart building systems. Collaborative efforts between industry and academia can facilitate the evolution of these models, ensuring that they remain at the forefront of building energy efficiency solutions. Continuous validation in diverse scenarios is crucial to maintain the relevance and accuracy of the results. The excellent performance of the M3 models, notably GPR-M3, in predicting building energy efficiency directly aligns with the United Nations' Sustainable Development Goals (SDGs), particularly Goal 7: Affordable and Clean Energy. By harnessing these models, we are not only advancing energy efficiency but also championing a sustainable, eco-friendly future. Their application could revolutionize the way we approach energy consumption, making strides towards more sustainable global infrastructure.

4.1. Interpretability of the Model (SHAP Analysis). Figure 10(a) showcases a SHAP (SHapley Additive exPlanations) plot detailing the influence of features on the ML model's prediction for GPR in determining which is the best model (HL). The vertical axis lists features such as RC, GA, and SA, while the horizontal axis denotes the SHAP value, capturing each feature's impact on the prediction. A central color gradient reveals the feature's actual value: pink for higher and blue for lower values. Notably, GA and SA exhibit a broad spread in SHAP values, signifying their pronounced influence on the model's outcomes. In contrast, features like OT, RA, and OH have minimal variation around the average prediction, indicating lesser influence. This comprehensive visualization underscores the differential impacts of each feature, pinpointing GA and SA as particularly significant contributors to the model's predictions.

For CL, the visualization is a SHAP plot, employed to communicate how individual features impact an ML model's predictions. On the vertical axis, we have features like RA, SA, GA, and more (see Figure 10(b)). The horizontal axis illustrates the SHAP value, reflecting each feature's influence on the model outcome: values to the right suggest a positive effect and values to the left suggest a negative effect. The color gradient, ranging from high (pink) to low (blue), represents the actual value of the feature for each data instance.

The dots across the graph are individual data points. Features like RA and SA predominantly lean to the right, indicating that when their values are high (represented by pink dots), they typically have a positive effect on the model's prediction. Conversely, for WA and RC, high values (again, pink dots) seem to push the prediction to the left, indicating a negative effect. Notably, the feature GA presents mixed results: high values of GA can be seen on both sides of the SHAP value, suggesting that it can either increase or decrease the model's prediction based on the context and presence of other features. The base value, delineated on the horizontal axis, represents the model's average prediction across the dataset. This visualization aids in deciphering how distinct features drive predictions away from this base value, underscoring the nuanced roles that each feature plays in the model's decision-making process.

Similarly, SHAP analysis significantly enhances the interpretability of AI models, aligning closely with the research objectives of advancing energy performance efficiency in residential buildings for sustainable design. By providing transparency in model decision-making, SHAP analysis reveals how different features, such as insulation quality or window orientation, impact heating load (HL) and cooling load (CL). This insight allows architects and planners to make data-driven design decisions, prioritizing the elements that most significantly contribute to energy efficiency. The identification of key predictors for energy efficiency through SHAP analysis is crucial in fine-tuning building designs to reduce energy consumption and in strategizing retrofitting existing buildings. Additionally, the explainability provided by SHAP analysis enhances the trustworthiness of the AI models among stakeholders, ensuring that model recommendations are more likely to be accepted and acted upon. These insights from SHAP analysis can also provide direction for future research in sustainable building design, focusing on areas with significant impacts on energy efficiency. This approach not only aids in minimizing energy consumption but also aligns with broader sustainability goals, such as those outlined in the United Nations' Sustainable Development Goals. Thus, SHAP analysis is integral in linking AI model interpretability to practical applications in sustainable building design while adopting informed, transparent, and effective strategies for enhancing energy efficiency.

5. Conclusion

This comprehensive study focused on evaluating and optimizing energy efficiency in residential buildings, leveraging various advanced ML models, specifically HLCL, to accurately estimate building energy performance, thereby ensuring optimum utilization of energy. The proposed model employed GPR, ENN, and BT algorithms, each with three input variables (M1-M3), explaining their capabilities in forecasting energy performance. Consistently across the models, the results reveal that the third combination, M3, consistently outperformed both M1 and M2. In particular, the GPR-M3 model showcased superior prediction skills in forecasting both heating and cooling loads. However, subtle

differences across the models became apparent, underscoring the need for diverse strategies depending on the focus, whether precision or broader prediction trends when measured with metrics such as MAPE and MAE. This demonstrates that the findings seamlessly align with the SDGs, particularly in championing sustainable cities and communities. To ensure the long-term efficacy and relevance of the models, continuous monitoring, feedback, and iterative refinements are essential. This will ensure that as building designs and technologies evolve, the models remain relevant and accurate. Based on the results and discussion, future research directions in this field could focus on several key areas:

(i) While the current study focuses on residential buildings, future research could extend these AI models to commercial, industrial, and institutional buildings. Additionally, testing these models in various climatic and geographical settings could provide a more comprehensive understanding of their applicability and effectiveness

(ii) Exploring how these AI models could be integrated with renewable energy sources (like solar or wind power) in building designs could offer insights into creating more sustainable and self-sufficient buildings

(iii) Implementing these models in real-time energy management systems could allow for predictive maintenance and more efficient energy use in buildings. This could include real-time adjustments to heating and cooling systems based on current occupancy and weather conditions

(iv) Researching how human behavior and occupancy patterns influence building energy consumption could refine these models further. This includes studying the impact of different lifestyles, work-from-home trends, and occupancy schedules on energy efficiency

(v) Investigating the role of innovative construction materials and techniques in enhancing building energy efficiency. This research could focus on how different materials and designs affect heating and cooling loads and how AI models can optimize these factors

(vi) Understanding how the findings from these AI models can inform and shape energy policies and building regulations. This could help governments and regulatory bodies implement standards and incentives that promote energy-efficient building designs

(vii) Conducting comprehensive analyses of the economic and environmental impacts of implementing these AI models in building design and construction. This includes cost-benefit analysis, lifecycle assessment, and carbon footprint analysis

(viii) Encouraging collaboration between architects, engineers, AI researchers, and environmental scientists to develop holistic and sustainable building solutions. This could lead to innovative designs that are both aesthetically pleasing and energy-efficient

(ix) Further exploration into how explainable AI can be made more accessible and understandable to architects, builders, and laypersons. This could involve developing user-friendly interfaces and visualization tools

(x) Conducting longitudinal studies to assess the long-term performance and durability of AI-optimized buildings. This would help in understanding how these buildings fare over time in terms of energy efficiency and structural integrity

Abbreviations

AI:	Artificial intelligence
AIX:	Explainable AI
ANN:	Artificial neural network
BT:	Boosted tree
CL:	Cooling load
MARS:	Multivariate adaptive regression splines
ENN:	Emotional neural learning
GA:	Glazing area
GD:	Glazing area distribution
GPR:	Gaussian process regression
HL:	Heating load
IoT:	Internet of Things
KNN:	K-nearest neighbors
MAE:	Mean absolute error
MAPE:	Mean absolute percentage error
ML:	Machine learning
OH:	Overall height
OT:	Orientation
PCC:	Pearson correlation coefficient
PLS:	Polynomial least square regression
RC:	Relative compactness
RF:	Random forest
SA:	Surface area
SDGs:	Sustainable Development Goals
SHAP:	SHapley Additive exPlanations
SVR:	Support vector regression
WA:	Wall area.

Data Availability

Data is available on request.

Conflicts of Interest

The author declares no conflict of interest.

Acknowledgments

References

[1] M. A. Majid, "Renewable energy for sustainable development in India: current status, future prospects, challenges, employment, and investment opportunities," *Energy, Sustainability and Society*, vol. 10, no. 1, pp. 1–36, 2020.

[2] B. A. Salami, S. I. Abba, A. A. Adewumi, U. A. Dodo, G. K. Otukogbe, and L. O. Oyedele, "Building energy loads prediction using Bayesian-based metaheuristic optimized-explainable tree-based model," *Case Studies in Construction Materials*, vol. 19, article e02676, 2023.

[3] S. B. Sadineni, S. Madala, and R. F. Boehm, "Passive building energy savings: a review of building envelope components," *Renewable and Sustainable Energy Reviews*, vol. 15, no. 8, pp. 3617–3631, 2011.

[4] L. Pérez-Lombard, J. Ortiz, J. F. Coronel, and I. R. Maestre, "A review of HVAC systems requirements in building energy regulations," *Energy and Buildings*, vol. 43, no. 2–3, pp. 255–268, 2011.

[5] Z. Hao, J. Xie, X. Zhang, and J. Liu, "Simplified model of heat load prediction and its application in estimation of building envelope thermal performance," *Buildings*, vol. 13, no. 4, p. 1076, 2023.

[6] G. Barone, A. Buonomano, C. Forzano, G. F. Giuzio, A. Palombo, and G. Russo, "A new thermal comfort model based on physiological parameters for the smart design and control of energy-efficient HVAC systems," *Renewable and Sustainable Energy Reviews*, vol. 173, article 113015, 2023.

[7] M. Y. Cheng and M. T. Cao, "Accurately predicting building energy performance using evolutionary multivariate adaptive regression splines," *Applied Soft Computing*, vol. 22, pp. 178–188, 2014.

[8] K. Kavaklioglu, "Robust modeling of heating and cooling loads using partial least squares towards efficient residential building design," *Journal of Building Engineering*, vol. 18, pp. 467–475, 2018.

[9] T. Yang, Y. Ding, B. Li, and A. K. Athienitis, "A review of climate adaptation of phase change material incorporated in building envelopes for passive energy conservation," *Building and Environment*, vol. 244, article 110711, 2023.

[10] R. Gupta, J. Mathur, and V. Garg, "Assessment of climate classification methodologies used in building energy efficiency sector," *Energy and Buildings*, vol. 298, article 113549, 2023.

[11] Y. Jung and M. Joo, "Building information modelling (BIM) framework for practical implementation," *Automation in Construction*, vol. 20, no. 2, pp. 126–133, 2011.

[12] J. Min, G. Yan, A. M. Abed et al., "The effect of carbon dioxide emissions on the building energy efficiency," *Fuel*, vol. 326, article 124842, 2022.

[13] T. P. Fowdur and B. Doorgakant, "A review of machine learning techniques for enhanced energy efficient 5G and 6G communications," *Engineering Applications of Artificial Intelligence*, vol. 122, article 106032, 2023.

[14] A. Valencia-Arias, V. García-Pineda, J. D. González-Ruiz, C. J. Medina-Valderrama, and R. Bao García, "Machine-learning applications in energy efficiency: a bibliometric approach and research agenda," *Designs*, vol. 7, no. 3, p. 71, 2023.

[15] W. A. Owusu and S. A. Marfo, "Artificial intelligence application in bioethanol production," *International Journal of Energy Research*, vol. 2023, Article ID 7844835, 8 pages, 2023.

[16] I. Talib, M. Yasin, J. Hussain, and R. Uwamahoro, "Performance evaluation and parametric optimization of coal-fired water tube boiler using the Grey-Taguchi method," *International Journal of Energy Research*, vol. 2023, Article ID 4203176, 11 pages, 2023.

[17] Z. Chen, F. Xiao, F. Guo, and J. Yan, "Interpretable machine learning for building energy management: a state-of-the-art review," *Advances in Applied Energy*, vol. 9, article 100123, 2023.

[18] B. Dong, C. Cao, and S. E. Lee, "Applying support vector machines to predict building energy consumption in tropical region," *Energy and Buildings*, vol. 37, no. 5, pp. 545–553, 2005.

[19] Z. Yu, F. Haghighat, B. C. M. Fung, and H. Yoshino, "A decision tree method for building energy demand modeling," *Energy and Buildings*, vol. 42, no. 10, pp. 1637–1646, 2010.

[20] J. Zhang and F. Haghighat, "Development of artificial neural network based heat convection algorithm for thermal simulation of large rectangular cross-sectional area earth-to-air heat exchangers," *Energy and Buildings*, vol. 42, no. 4, pp. 435–440, 2010.

[21] M. Nilashi, M. Dalvi-Esfahani, O. Ibrahim, K. Bagherifard, A. Mardani, and N. Zakuan, "A soft computing method for the prediction of energy performance of residential buildings," *Measurement*, vol. 109, pp. 268–280, 2017.

[22] S. Sekhar Roy, R. Roy, and V. E. Balas, "Estimating heating load in buildings using multivariate adaptive regression splines, extreme learning machine, a hybrid model of MARS and ELM," *Renewable and Sustainable Energy Reviews*, vol. 82, pp. 4256–4268, 2018.

[23] T. X. Dan and P. N. K. Phuc, "Application of machine learning in forecasting energy usage of building design," in *2018 4th International Conference on Green Technology and Sustainable Development (GTSD)*, pp. 53–59, Ho Chi Minh City, Vietnam, 2018.

[24] Q. Li, Q. Meng, J. Cai, H. Yoshino, and A. Mochida, "Predicting hourly cooling load in the building: a comparison of support vector machine and different artificial neural networks," *Energy Conversion and Management*, vol. 50, no. 1, pp. 90–96, 2009.

[25] Q. Li, Q. Meng, J. Cai, H. Yoshino, and A. Mochida, "Applying support vector machine to predict hourly cooling load in the building," *Applied Energy*, vol. 86, no. 10, pp. 2249–2256, 2009.

[26] R. K. Jain, K. M. Smith, P. J. Culligan, and J. E. Taylor, "Forecasting energy consumption of multi-family residential buildings using support vector regression: investigating the impact of temporal and spatial monitoring granularity on performance accuracy," *Applied Energy*, vol. 123, pp. 168–178, 2014.

[27] A. Entezari, A. Aslani, R. Zahedi, and Y. Noorollahi, "Artificial intelligence and machine learning in energy systems: a bibliographic perspective," *Energy Strategy Reviews*, vol. 45, article 101017, 2023.

[28] J. S. Chou and D. K. Bui, "Modeling heating and cooling loads by artificial intelligence for energy-efficient building design," *Energy and Buildings*, vol. 82, pp. 437–446, 2014.

[29] L. A. López-Pérez and J. J. Flores-Prieto, "Adaptive thermal comfort approach to save energy in tropical climate educational building by artificial intelligence," *Energy*, vol. 263, article 125706, 2023.

[30] R. Olu-Ajayi, H. Alaka, I. Sulaimon, F. Sunmola, and S. Ajayi, "Building energy consumption prediction for residential buildings using deep learning and other machine learning techniques," *Journal of Building Engineering*, vol. 45, article 103406, 2022.

[31] T. Saheb, M. Dehghani, and T. Saheb, "Artificial intelligence for sustainable energy: a contextual topic modeling and content analysis," *Sustainable Computing: Informatics and Systems*, vol. 35, article 100699, 2022.

[32] A. I. Dounis, "Artificial intelligence for energy conservation in buildings," *Advances in Building Energy Research*, vol. 4, no. 1, pp. 267–299, 2010.

[33] R. Machlev, L. Heistrene, M. Perl et al., "Explainable artificial intelligence (XAI) techniques for energy and power systems: review, challenges and opportunities," *Energy and AI*, vol. 9, article 100169, 2022.

[34] S. I. Abba, J. C. Egbueri, M. Benaafi, J. Usman, A. G. Usman, and I. H. Aljundi, "Fluoride and nitrate enrichment in coastal aquifers of the Eastern Province, Saudi Arabia: The influencing factors, toxicity, and human health risks," *Chemosphere*, vol. 336, article 139083, 2023.

[35] R. Costache, Q. B. Pham, E. Sharifi et al., "Flash-flood susceptibility assessment using multi-criteria decision making and machine learning supported by remote sensing and GIS techniques," *Remote Sensing*, vol. 12, no. 1, p. 106, 2020.

[36] B. S. Alotaibi, K. R. M. Khalifa, M. A. Abuhussain et al., "Integrating renewable-based solar energy into sustainable and resilient urban furniture coupled with a logical multi-comparison study of Cyprus and Saudi Arabia," *Processes*, vol. 11, no. 10, p. 2887, 2023.

[37] B. S. Alotaibi, M. S. Yahuza, O. Ozden et al., "Sustainable green building awareness: a case study of Kano integrated with a representative comparison of Saudi Arabian Green Construction," *Buildings*, vol. 13, no. 9, p. 2387, 2023.

[38] A. Tsanas and A. Xifara, "Accurate quantitative estimation of energy performance of residential buildings using statistical machine learning tools," *Energy and Buildings*, vol. 49, pp. 560–567, 2012.

[39] F. E. Sapnken, M. M. Hamed, B. Soldo, and J. Gaston Tamba, "Modeling energy-efficient building loads using machine-learning algorithms for the design phase," *Energy and Buildings*, vol. 283, article 112807, 2023.

[40] H. M. Baalousha, A. Younes, M. A. Yassin, and M. Fahs, "Comparison of the fuzzy analytic hierarchy process (F-AHP) and fuzzy logic for flood exposure risk assessment in arid regions," *Hydrology*, vol. 10, no. 7, p. 136, 2023.

[41] S. I. Abba, Q. B. Pham, G. Saini et al., "Implementation of data intelligence models coupled with ensemble machine learning for prediction of water quality index," *Environmental Science and Pollution Research*, vol. 27, no. 33, pp. 41524–41539, 2020.

[42] M. A. Yassin, A. G. Usman, S. I. Abba, D. U. Ozsahin, and I. H. Aljundi, "Intelligent learning algorithms integrated with feature engineering for sustainable groundwater salinization modelling: Eastern Province of Saudi Arabia," *Results in Engineering*, vol. 20, article 101434, 2023.

[43] A. G. Usman, S. Işik, and S. I. Abba, "hybrid data-intelligence algorithms for the simulation of thymoquinone in HPLC method development," *Journal of the Iranian Chemical Society*, vol. 18, no. 7, pp. 1537–1549, 2021.

[44] M. A. Yassin, B. Tawabini, A. Al-Shaibani et al., "Geochemical and spatial distribution of topsoil HMs coupled with modeling of Cr using Chemometrics intelligent techniques: case study from Dammam Area, Saudi Arabia," *Molecules*, vol. 27, no. 13, p. 4220, 2022.

[45] A. G. Usman, S. Işik, S. I. Abba, and F. Meriçli, "Chemometrics-based models hyphenated with ensemble machine learning for retention time simulation of isoquercitrin in Coriander sativum L. using high-performance liquid chromatography," *Journal of Separation Science*, vol. 44, no. 4, pp. 843–849, 2021.

[46] M. Benaafi, M. A. Yassin, A. G. Usman, and S. I. Abba, "Neurocomputing modelling of hydrochemical and physical properties of groundwater coupled with spatial clustering, GIS, and statistical techniques," *Sustainability*, vol. 14, no. 4, p. 2250, 2022.

[47] D. Nunno, F. S. I. Abba, B. Quoc, P. Abu, R. Towfiqul, and I. Swapan, "Groundwater level forecasting in northern Bangladesh using nonlinear autoregressive exogenous (NARX) and extreme learning machine (ELM) neural networks," *Arabian Journal of Geosciences*, vol. 15, no. 7, pp. 1–20, 2022.

[48] B. Mohammadi, N. T. T. Linh, Q. B. Pham et al., "Adaptive neuro-fuzzy inference system coupled with shuffled frog leaping algorithm for predicting river streamflow time series," *Hydrological Sciences Journal*, vol. 65, no. 10, pp. 1738–1751, 2020.

[49] Q. B. Pham, S. S. Sammen, S. I. Abba, B. Mohammadi, S. Shahid, and R. A. Abdulkadir, "A new hybrid model based on relevance vector machine with flower pollination algorithm for phycocyanin pigment concentration estimation," *Environmental Science and Pollution Research*, vol. 28, no. 25, pp. 32564–32579, 2021.

[50] H. Tao, M. M. Hameed, H. A. Marhoon et al., "Groundwater level prediction using machine learning models: a comprehensive review," *Neurocomputing*, vol. 489, pp. 271–308, 2022.

[51] S. Heddam, H. Lamda, and S. Filali, "Predicting effluent biochemical oxygen demand in a wastewater treatment plant using generalized regression neural network based approach: a comparative study," *Environmental Processes*, vol. 3, no. 1, pp. 153–165, 2016.

[52] Z. M. Yaseen, W. H. M. W. Mohtar, A. M. S. Ameen et al., "Implementation of univariate paradigm for streamflow simulation using hybrid data-driven model: case study in tropical region," *IEEE Access*, vol. 7, pp. 74471–74481, 2019.

[53] Z. M. Yaseen, I. Ebtehaj, H. Bonakdari et al., "Novel approach for streamflow forecasting using a hybrid ANFIS-FFA model," *Journal of Hydrology*, vol. 554, pp. 263–276, 2017.

[54] A. G. Usman, S. Işik, and S. I. Abba, "A novel multi-model data-driven ensemble technique for the prediction of retention factor in HPLC method development," *Chromatographia*, vol. 83, no. 8, pp. 933–945, 2020.

[55] A. Malik, Y. Tikhamarine, S. S. Sammen, S. I. Abba, and S. Shahid, "Prediction of meteorological drought by using hybrid support vector regression optimized with HHO versus PSO algorithms," vol. 28, no. 29, pp. 39139–39158, 2021.

[56] M. Al-Maas, A. Hussain, J. M. Matar et al., "Validation and application of a membrane filtration evaluation protocol for oil-water separation," *Journal of Water Process Engineering*, vol. 43, article 102185, 2021.

[57] R. G. Sargent, "Verification and validation of simulation models," in *Proceedings of the 2009 Winter Simulation Conference (WSC)*, pp. 162–176, Austin, TX, USA, 2009.

[58] H. Cai, X. Jia, J. Feng, W. Li, Y. M. Hsu, and J. Lee, "Gaussian process regression for numerical wind speed prediction enhancement," *Renewable Energy*, vol. 146, pp. 2112–2123, 2020.

[59] E. Momeni, M. B. Dowlatshahi, F. Omidinasab, H. Maizir, and D. J. Armaghani, "Gaussian process regression technique to

estimate the pile bearing capacity," *Arabian Journal for Science and Engineering*, vol. 45, no. 10, pp. 8255–8267, 2020.

[60] Y. Lu, J. Ma, L. Fang, X. Tian, and J. Jiang, "Robust and scalable Gaussian process regression and its applications," in *Proceedings of the IEEE/CVF Conference on Computer Vision and Pattern Recognition*, pp. 21950–21959, Vancouver, BC, Canada, 2023.

[61] M. Gashler, C. Giraud-Carrier, and T. Martinez, "Decision tree ensemble: small heterogeneous is better than large homogeneous," in *2008 Seventh International Conference on Machine Learning and Applications*, pp. 900–905, San Diego, CA, USA, 2008.

[62] H. Mohammed, I. A. Hameed, and R. Seidu, "Random forest tree for predicting fecal indicator organisms in drinking water supply," in *2017 International Conference on Behavioral, Economic, Socio-cultural Computing (BESC)*, pp. 1–6, Krakow, Poland, 2017.

[63] I. D. Mienye, Y. Sun, and Z. Wang, "Prediction performance of improved decision tree-based algorithms: a review," *Procedia Manufacturing*, vol. 35, pp. 698–703, 2019.

[64] S. Kumar, T. Roshni, and D. Himayoun, "A comparison of emotional neural network (ENN) and artificial neural network (ANN) approach for rainfall-runoff modelling," *Civil Engineering Journal*, vol. 5, no. 10, pp. 2120–2130, 2019.

[65] V. Nourani, A. Molajou, S. Uzelaltinbulat, and F. Sadikoglu, "Emotional artificial neural networks (EANNs) for multi-step ahead prediction of monthly precipitation; case study: northern Cyprus," *Theoretical and Applied Climatology*, vol. 138, no. 3–4, pp. 1419–1434, 2019.

[66] S. I. Haruna, S. I. Malami, M. Adamu et al., "Compressive strength of self-compacting concrete modified with rice husk ash and calcium carbide waste modeling: a feasibility of emerging emotional intelligent model (EANN) versus traditional FFNN," *Arabian Journal for Science and Engineering*, vol. 46, no. 11, pp. 11207–11222, 2021.

[67] S. I. Abba, R. A. Abdulkadir, S. S. Sammen et al., "Integrating feature extraction approaches with hybrid emotional neural networks for water quality index modeling," *Applied Soft Computing*, vol. 114, article 108036, 2022.

[68] E. Lotfi and M. R. Akbarzadeh-T, "Practical emotional neural networks," *Neural Networks*, vol. 59, pp. 61–72, 2014.

[69] A. Khashman, "Application of an emotional neural network to facial recognition," *Neural Computing and Applications*, vol. 18, no. 4, pp. 309–320, 2009.

[70] A. U. Muhammad, X. Li, and J. Feng, "Using LSTM GRU and Hybrid Models for Streamflow Forecasting," in *Machine Learning and Intelligent Communications. MLICOM 2019*, X. Zhai, B. Chen, and K. Zhu, Eds., vol. 294 of Lecture Notes of the Institute for Computer Sciences, Social Informatics and Telecommunications Engineering, Springer, Cham, 2019.

[71] N. Baig, J. Usman, S. I. Abba, M. Benaafi, and I. H. Aljundi, "Fractionation of dyes/salts using loose nanofiltration membranes: insight from machine learning prediction," *Journal of Cleaner Production*, vol. 418, article 138193, 2023.

[72] N. Baig, S. I. Abba, J. Usman, M. Benaafi, and I. H. Aljundi, "Ensemble hybrid machine learning to simulate dye/divalent salt fractionation using a loose nanofiltration membrane," *Environmental Science: Advances*, vol. 2, no. 10, pp. 1446–1459, 2023.